

# Lawrence Berkeley National Laboratory

## LBL Publications

### Title

Extension of TOUGH-FLAC to the finite strain framework

### Permalink

<https://escholarship.org/uc/item/7865j9kr>

### Authors

Blanco-Martín, Laura  
Rutqvist, Jonny  
Birkholzer, Jens T

### Publication Date

2017-11-01

### DOI

10.1016/j.cageo.2016.10.015

Peer reviewed

# Extension of TOUGH-FLAC to the finite strain framework

Laura Blanco-Martín, Jonny Rutqvist, Jens T. Birkholzer

## Abstract

The TOUGH-FLAC simulator for coupled thermal-hydraulic-mechanical processes modeling has been extended to the finite strain framework. In the approach selected, this extension has required modifications to the flow simulator (TOUGH2) and to the coupling scheme between the geomechanics and the flow sub-problems. In TOUGH2, the mass and energy balance equations have been extended to account for volume changes. Additionally, as large deformations are computed by FLAC<sup>3D</sup>, the geometry is updated in the flow sub-problem. The Voronoi partition needed in TOUGH2 is computed using an external open source library (Voro++) that uses the centroids of the deformed geomechanics mesh as generators of the Voronoi diagram. TOUGH-FLAC in infinitesimal and finite strain frameworks is verified against analytical solutions and other approaches to couple flow and geomechanics. Within the finite strain framework, TOUGH-FLAC is also successfully applied to a large-scale case. The extension of TOUGH-FLAC to the finite strain framework has little impact to the user as only one additional executable is needed (for Voro++), and the input files and the workflow of a simulation are the same as in standard TOUGH-FLAC. With this new provision for finite strains, TOUGH-FLAC can be used in the analysis of a wider range of engineering problems, and the areas of application of this simulator are therefore broadened.

Keywords: Finite strains, Coupled THM processes, TOUGH2, FLAC<sup>3D</sup>, Sequential modeling, Voro++

## 1. Introduction

Geoenergy and geoenvironmental applications in the subsurface often require that the coupling between different processes be considered. Typical examples of such applications are geological carbon sequestration, enhanced geothermal systems, oil/gas production, compressed air energy storage and underground disposal of nuclear waste. While in some cases coupling between hydraulic and mechanical processes may be sufficient to capture the main features of the coupled system (changes in effective stresses due to pore pressure changes and porosity changes due to volumetric deformation), in many cases the interactions need to be extended to thermal, chemical and possibly other (biological, etc.) processes.

In this study, we focus on coupled thermal-hydraulic-mechanical (THM) processes, for which two main solution approaches exist in the literature: fully coupled and sequentially coupled (Dean et al., 2006, Kim et al., 2009). In fully coupled methods, the governing equations of each sub-problem (i.e., mass and heat flows, and geomechanics) are solved simultaneously in a single system of equations. In sequential methods, the governing equations for flow and geomechanics are solved one-by-one within a time step, and

relevant information (pore pressure, volumetric deformation, temperature, etc.) is passed from one sub-problem to the other using an intermediate solution information technique (Settari and Mourits, 1998). The main advantage of fully coupled approaches is that they are unconditionally stable and converge if the coupled problem is well-posed; on the other hand, they require a unified flow-geomechanics simulator and are computationally expensive due to the size of the system of equations to be solved. In turn, sequentially coupled methods are less computationally intensive, provide more flexible code management, offer the possibility to use existing codes for flow and geomechanics, and can use different spatial domains for each sub-problem. Additionally, the converged solution is identical to that obtained using the fully coupled approach (Kim et al., 2009).

The sequential simulator TOUGH-FLAC was presented in the TOUGH Symposium 2003 as a new tool to solve coupled flow and geomechanics processes (Rutqvist et al., 2002; Rutqvist and Tsang, 2003). Since then, the capabilities of this simulator have been augmented considerably, and at present it can be successfully applied to a wide range of applications (Rutqvist, 2011, Rutqvist, 2015). As the name suggests, in TOUGH-FLAC the multiphase, multicomponent and non-isothermal flow sub-problem is computed by TOUGH2 (Transport of Unsaturated Groundwater and Heat, v2, Pruess et al. (2012)), and the geomechanics sub-problem is computed by FLAC<sup>3D</sup>(Fast Lagrangian Analysis of Continua in 3D, Itasca (2012)). TOUGH2 is an integral finite difference code and FLAC<sup>3D</sup> is a finite difference code. In addition to its flexibility to be used in a broad variety of applications, one main advantage of TOUGH-FLAC is that both TOUGH2 and FLAC<sup>3D</sup> are used in both academia and industry, and are under constant development.

Recently, TOUGH-FLAC was extended to the finite strain framework (Blanco-Martín et al., 2015a, Blanco-Martín et al., 2015b). This extension was motivated by the distortions and deformations observed in some applications, which exceed the limits of validity of the infinitesimal strain theory. For instance, the disposal of heat-generating nuclear waste in rock salt is expected to entail significant configuration changes: salt creeps and distorts under the effect of temperature and deviatoric stresses, and if damage and/or sealing occur(s), significant volume changes may take place (Hunsche and Hampel, 1999). Furthermore, compaction and dilation of geomaterials also involve large deformations. Still in the context of nuclear waste disposal in rock salt, the backfill material (crushed salt) is expected to undergo a reconsolidation process, in which its initial porosity (30–40%) reduces progressively to low residual values (<10%), thereby triggering significant geometrical changes (Kröhn et al., 2015). Additionally, finite strains are common in oceanic gas hydrate reservoirs (Moridis et al., 2013).

In this paper, we summarize the architecture of TOUGH-FLAC and the modifications performed to extend this simulator to the finite strain framework. Then, we present some validation tests, first in infinitesimal mode, and later in large strain mode. Finally, we present a large-scale

application in which TOUGH-FLAC in finite strains is successfully applied. The extension of TOUGH-FLAC to the finite strain framework widens the range of engineering problems that can be studied with this simulator and therefore broadens its areas of application.

## 2. Materials and methods

### 2.1. Architecture of TOUGH-FLAC

TOUGH-FLAC is based on the fixed-stress split sequential method to couple flow and geomechanics (Kim et al., 2009). In this method, the flow sub-problem is solved first within a time step. Once convergence has been reached in TOUGH2 (Newton-Raphson iteration process to solve mass and heat balances), relevant information (pore pressure, temperature and fluid mass) is sent to FLAC<sup>3D</sup> to compute geomechanical equilibrium under drained conditions. Fluid mass is used to update the total mass of the system. The total stress tensor is updated using (direct coupling)

$$\sigma_{ij}^{corr} = \sigma_{ij} - \alpha \Delta P \delta_{ij} - 3\alpha_{th} K \Delta T \delta_{ij} \quad (1)$$

where  $\sigma_{ij}^{corr}$  [MPa] is the updated total stress tensor,  $\sigma_{ij}$  [MPa] is the total stress tensor at the end of the previous FLAC<sup>3D</sup>run,  $\alpha$  [-] is the Biot coefficient,  $\Delta P$  [MPa] is the pore pressure change between two consecutive TOUGH2 runs,  $\alpha_{th}$  [K<sup>-1</sup>] is the linear thermal expansion coefficient,  $K$  [MPa] is the drained bulk modulus,  $\Delta T$  [K] is the temperature change between two consecutive TOUGH2 runs, and  $\delta_{ij}$  [-] is the Kronecker delta. Here, we consider that compressive stresses are negative. From Eq. (1), it can be inferred that the flow only affects the volumetric component of the stress tensor.

Pressure, temperature and fluid mass are transferred through text files handled by means of a THM interface, written both in Fortran (TOUGH2) and FISH (programming language embedded within FLAC<sup>3D</sup>). Although less efficient, this approach has been selected because the source code of FLAC<sup>3D</sup> is not available to users.

Within the framework of viscoelasticity or viscoplasticity, the time modeled in each FLAC<sup>3D</sup> call is equal to the time step size of the last converged TOUGH2 time step (in elasticity, the physical time does not take part in the mechanical response). In this case, FLAC<sup>3D</sup> splits the time to be modeled into smaller time steps, controlled internally to avoid exceedingly large out-of-balance forces. Once the system is in mechanical equilibrium, volumetric stresses of each zone are transferred to TOUGH2 by means of a text file; they will be used to compute a mechanically induced correction term in the porosity increment in the next flow time step (explicit evaluation). This increment reads

$$d\phi = A(\alpha, \phi, K)dP + B(\alpha_{th})dT + \Delta\phi \quad (2)$$

where  $\Delta\phi$  [-] is the porosity correction from geomechanics (details can be found in Kim et al. [2012]). Additionally, other variables can be transferred to compute mechanically induced changes in permeability and capillary pressure (indirect coupling, see Rutqvist (2011) for details). A new flow time step is then taken, and the procedure described is repeated until the end of the simulation.

## 2.2. Extension of TOUGH-FLAC to the finite strain framework

Strain changes are computed within the geomechanics sub-problem, and, if they are large enough, it is necessary to ensure that the flow sub-problem is consistently updated. While FLAC<sup>3D</sup> provides a capability for large strains, TOUGH2 does not. Therefore, in order to extend TOUGH-FLAC into the finite strain framework, it has been necessary to (i) adapt TOUGH2 to finite strains, and (ii) adapt the coupling between the two codes to the new framework.

Two main modifications have been necessary in TOUGH2. First, all geometrical data are updated as the geomechanics mesh deforms: volume of grid-blocks, interface area between two connected grid-blocks, distance from centers of two connected grid-blocks to common interface, and angle between the line linking two connected grid-blocks and the gravitational acceleration vector. Second, the heat and mass balance equations have been extended to include volume changes, and now read, for a grid-block  $n$ ,

$$\frac{d(M_n^\kappa V_n)}{dt} = \sum_m A_{nm} F_{nm}^\kappa + q_n^\kappa \rightarrow \frac{dM_n^\kappa}{dt} + M_n^\kappa \frac{dV_n}{V_n dt} = \frac{1}{V_n} (\sum_m A_{nm} F_{nm}^\kappa + q_n^\kappa) \quad (3)$$

for  $\kappa=1, NK+1$  ( $NK$  is the total number of fluid components [air, water, etc.], and  $NK+1$  represents the heat equation). In Eq. (3),  $M_n^\kappa$  is the accumulation term of component  $\kappa$  in grid-block  $n$ ,  $V_n$  [m<sup>3</sup>] is the volume of the grid block (new volume after each FLAC<sup>3D</sup> call),  $q_n^\kappa$  [kg/s or J/s] denotes sink/sources rates, and  $F_{nm}^\kappa$  is the flow of component  $\kappa$  across surface  $A_{nm}$  [m<sup>2</sup>] (new value after each FLAC<sup>3D</sup> call). Eq. (3) reduces to the standard balance equations by setting  $dV_n=0$ . The mass accumulation terms,  $M_n^\kappa$  [kg/m<sup>3</sup>], read

$$M_n^\kappa = \phi \sum_\beta S_\beta \rho_\beta \chi_{\beta\kappa} \quad (4)$$

In Eq. (4),  $S_\beta$  [-] is the saturation of phase  $\beta$ ,  $\rho_\beta$  [kg/m<sup>3</sup>] is the density of phase  $\beta$ , and  $\chi_{\beta\kappa}$  [-] is the mass fraction of component  $\kappa$  in phase  $\beta$ . The heat accumulation term,  $M_n^{NK+1}$  [J/m<sup>3</sup>], reads

$$M_n^{NK+1} = (1 - \phi)\rho_{gr}C_pT + \phi \sum_{\beta} S_{\beta}\rho_{\beta}u_{\beta} \quad (5)$$

where  $\rho_{gr}$  [kg/m<sup>3</sup>] is the rock grain density,  $C_p$  [J/kg/K] is the rock grain specific heat and  $u_{\beta}$  [J/kg] is the specific internal energy in phase  $\beta$ .

Mass transport occurs by advection and diffusion, so that the mass flux of component  $\kappa$ ,  $F_{nm\kappa}$  [kg/m<sup>2</sup>/s], reads

$$F_{nm}^{\kappa} = - \sum_{\beta} k \frac{k_{r\beta}\rho_{\beta}}{\mu_{\beta}} (\nabla P_{\beta} - \rho_{\beta}g) \chi_{\beta}^{\kappa} - \sum_{\beta} \rho_{\beta} D_{\beta}^{\kappa} \nabla \chi_{\beta}^{\kappa} \quad (6)$$

where  $k$  [m<sup>2</sup>] is the absolute permeability of the porous medium,  $k_{r\beta}$  [-] is the relative permeability to phase  $\beta$ ,  $\mu_{\beta}$  [Pa·s] is viscosity of phase  $\beta$ ,  $P_{\beta}$  [Pa] is phase pressure and  $g$  [m/s<sup>2</sup>] is the gravity acceleration vector. Regarding the diffusive term,  $D_{\beta}^{\kappa}$  [m<sup>2</sup>/s] is the hydrodynamic dispersion tensor of component  $\kappa$  in phase  $\beta$ , (see Pruess et al. (2012) for further details).

Finally, heat transport occurs by conduction and convection, and the heat flux term,  $F_{nm}^{\kappa}$  [J/m<sup>2</sup>/s], reads

$$F_{nm}^{NK+1} = -\lambda \nabla T - \sum_{\beta} k \frac{k_{r\beta}\rho_{\beta}}{\mu_{\beta}} (\nabla P_{\beta} - \rho_{\beta}g) h_{\beta} \quad (7)$$

where  $\lambda$  [W/m/K] is the thermal conductivity and  $h_{\beta}$  [J/kg] is the specific enthalpy in phase  $\beta$ .

Regarding the coupling between the two codes, the new geometrical data is transferred to TOUGH2 through a text file; this file is subsequently read by a new Fortran subroutine to update the corresponding geometrical arrays. We note that the main drawback of the approach selected to extend TOUGH-FLAC to the finite strain framework is an increase of computational time due to geometry update. An alternative approach would consist in keeping the geometry unchanged, and mapping relevant properties (such as permeability) onto the reference configuration; however, this approach requires full tensor (i.e., non-diagonal) permeability, and this is not supported in the current version of TOUGH2. For this reason, we selected an approach in which geometry is updated.

Fig. 1 shows the numerical scheme used in TOUGH-FLAC, including transfer of geometrical data. This scheme is also valid in creep mode (time-dependent geomechanical behavior). It should be noted that the general workflow of TOUGH-FLAC (Rutqvist, 2011) is not noticeably modified when finite strains are considered. Additionally, the impact for the user is minimal, as all modifications are taken care of internally. Only one additional

executable is needed to properly update the flow mesh (see next sub-section).

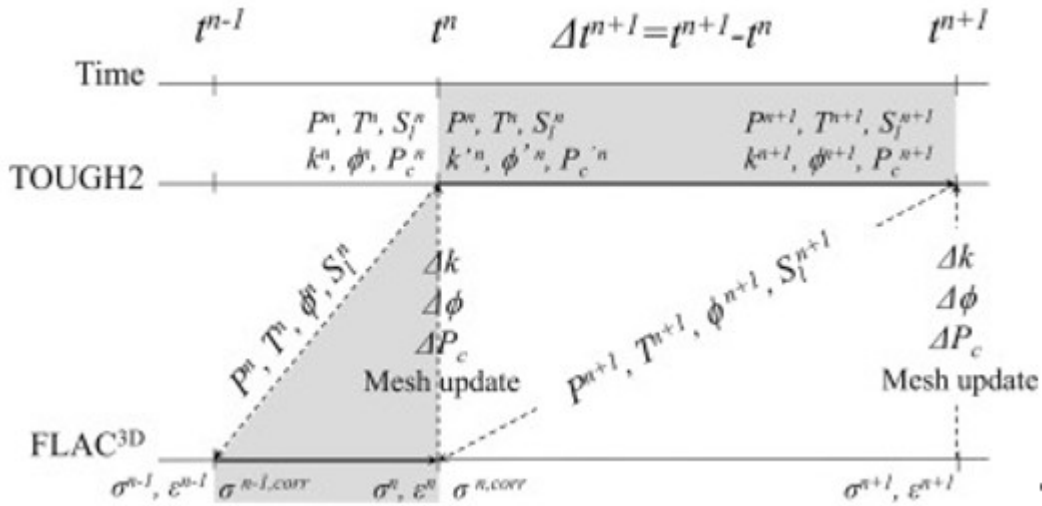


Fig. 1. TOUGH-FLAC numerical scheme in finite strains. The gray area corresponds to a time step between  $t^n$  and  $t^{n+1}$ .

### 2.3. Mesh update in the flow sub-problem

The resolution method used in TOUGH2 is based on the Voronoi partition (Pruess et al., 2012). As large deformations occur, the updated flow mesh should still be of Voronoi type for an accurate solution of the flow sub-problem. For this reason, we have linked the software library Voropp (Rycroft, 2009) to TOUGH-FLAC. Voropp is open source, and can compute 3D Voronoi partitions on a cell-based fashion. Moreover, customizing its output for a particular application is not time-consuming.

The new workflow to update the mesh in the flow sub-problem is as follows. First, the centroids of the deformed geomechanics mesh are transferred using a FISH routine to Voropp, which computes the corresponding Voronoi diagram. Then, data of the new partition relevant to TOUGH2 (volumes, distances, areas, etc.) are written into a text file. This file is finally read by TOUGH2, and the corresponding arrays are updated. In general, this operation is performed every time maximum volumetric strain changes are greater than 2–3%. We note however that this condition can be easily changed in the FISH routine written to transfer data to Voropp. For instance, in cases where the mesh distorts without significant volume changes, the flow mesh should be updated, as the interface areas, distances and angle between the line linking two connected grid-blocks and the gravity vector may change noticeably. Fig. 2 shows an example of a geomechanics mesh and the corresponding Voronoi partition, both in the non-deformed and deformed configurations.

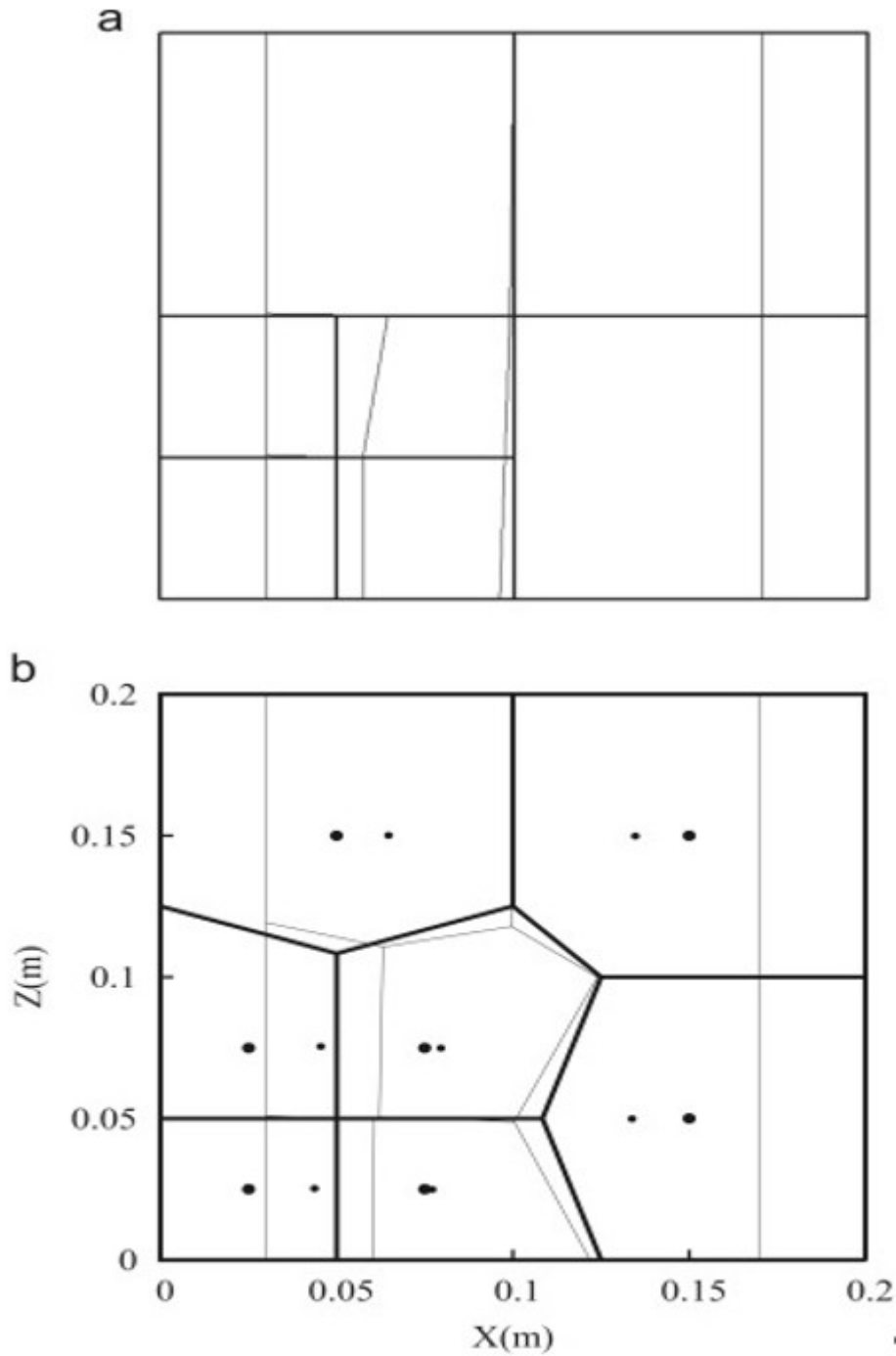


Fig. 2. Example of mesh used in the geomechanics sub-problem (a) and corresponding Voronoi partition for the flow sub-problem (b). Initial (thick lines) and deformed (thin lines) configurations are displayed.

### 3. Verification cases

In this section, TOUGH-FLAC is verified against classic analytical solutions of coupled problems, and it is also benchmarked against other simulators that can handle finite strains. The first three cases presented are related to well-



known benchmark problems in small strains, which demonstrate the correct coupling between TOUGH2 and FLAC<sup>3D</sup> prior to addressing finite strains.

### 3.1. Mandel's problem (small strains)

Mandel's problem is commonly used to test the validity of numerical codes of poroelasticity. The original problem is described in Mandel (1953). Later, this problem was extended to account for non-isotropic materials as well as compressible fluids (Abousleiman et al., 1996).

In Mandel's problem, a specimen with rectangular cross-section and infinite length along the out-of-plane direction is sandwiched at the top and the bottom by two stiff, frictionless plates. The pore space is in single-phase conditions. Laterally, the specimen is not mechanically constrained, and drainage is possible (no drainage at the top and bottom). The specimen is initially in equilibrium. At  $t=0$ , a compressive force is applied normal to the plates, and we seek to determine the evolution of pore pressure, as well as relevant displacements, strains and stresses within the sample. Fig. 3 shows a schematic representation of Mandel's problem.

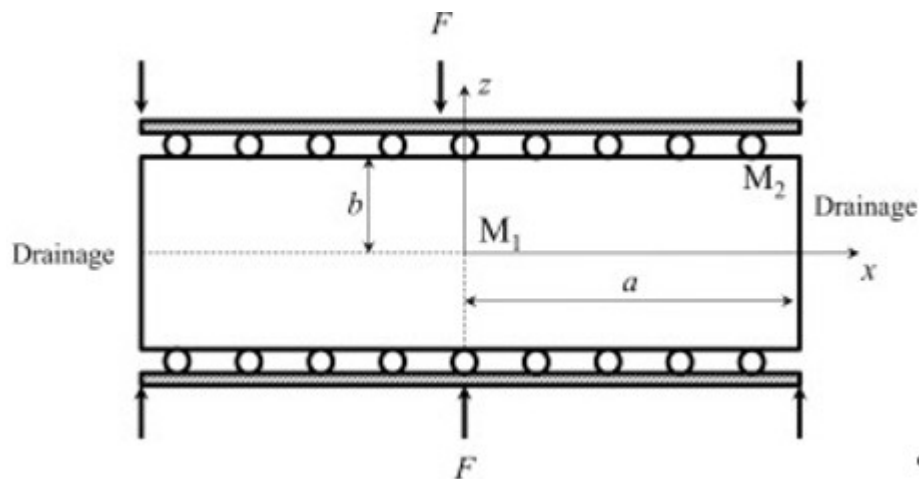


Fig. 3. Schematic representation of Mandel's problem. Monitoring points ( $M_1$  and  $M_2$ ) for Fig. 4 are displayed.

Mandel's problem is a two-dimensional, plane strain problem. Because the plates are perfectly stiff, the vertical displacement is uniform along the top and bottom boundaries (but it changes with time). When the load is applied, an excess of pore pressure is generated (Skempton effect). Over time, drainage occurs at the open boundaries, which makes the laterals of the sample more compliant than its core. However, since the vertical displacement must be equal along the top and bottom boundaries, there is an increase of pore pressure in the central region. This yields a non-monotonic pore pressure evolution, known as the Mandel-Cryer effect (Schiffman et al., 1969). At a later time, the excess of pore pressure dissipates completely throughout the sample. We note that the Mandel-Cryer effect has been observed experimentally (Verruijt, 1969).

Mandel's problem has been modeled with TOUGH-FLAC. We have assumed a sample with  $a = 5$  m,  $b = 1.25$  m,  $E = 450$  MPa, and  $\nu = 0$ . The initial stress field is 0.1 MPa (compressive), and we apply 10 MPa normal to the plates. The initial porosity is  $\phi_0 = 42.5\%$  and the permeability of the sample is  $k = 6.51 \cdot 10^{-15}$  m<sup>2</sup>. The sample is saturated with water, having  $T = 25$  °C (constant) and  $p_0 = 0.1$  MPa. Gravity is neglected. Given that TOUGH2 accounts for fluid compressibility changes, we have compared our modeling results with the analytical solution proposed by Abousleiman et al. (1996). Furthermore, in order to model frictionless plates, an interface is used between the sample and the plates.

The plots in Fig. 4 compare analytical and modeling results at the locations displayed in Fig. 3. As the figure shows, the comparisons are very satisfactory (note that the differences observed at the beginning are due to different initial states: in the analytical solution, the load is already applied and borne by the fluid, and the corresponding excess is calculated; on the other hand, in TOUGH-FLAC the initial state corresponds to a previous state of equilibrium, and at  $t = 0$  the load is applied to the sample). These results help verify the validity of TOUGH-FLAC to solve coupled flow and geomechanics problems.

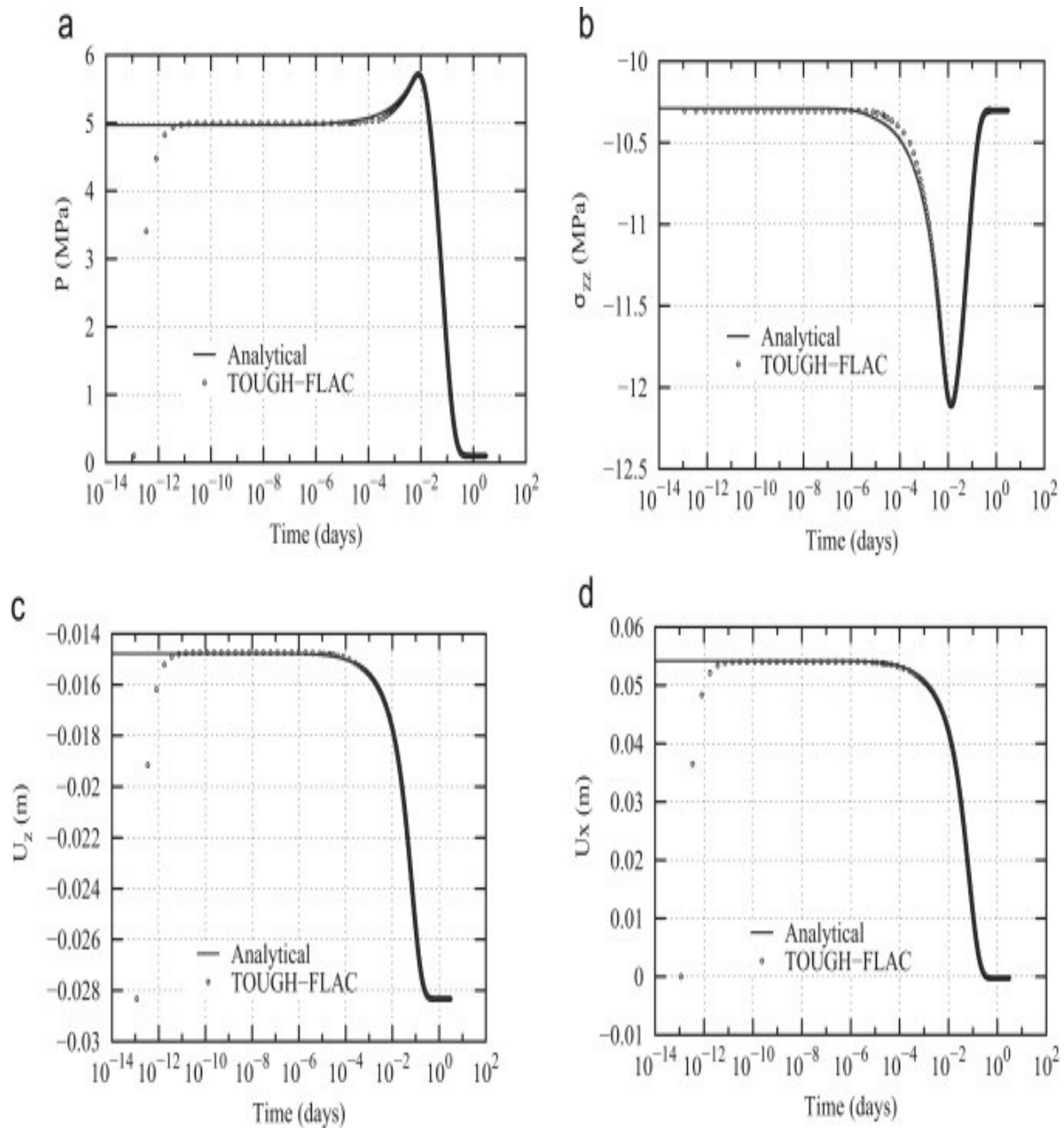


Fig. 4. Mandel's problem: comparison between analytical and modeling results for (a) pore pressure at  $M_1$ ; (b) vertical stress at  $M_1$ ; (c) vertical displacement at  $M_2$ , and (d) horizontal displacement at  $M_2$ .

### 3.2. Booker and Savvidou's problem (small strains)

Booker and Savvidou (1985) proposed an analytical solution for a problem involving a point heat source buried in a saturated medium. This configuration is characteristic of the underground disposal of heat-generating nuclear waste. The analytical solution was developed assuming a poro-thermo elastic medium, and has been used to test the validity of THM codes (Nguyen and Selvadurai, 1995).

In Booker and Savvidou's problem, a saturated, infinite medium is initially in equilibrium. At  $t=0$ , a heat load is applied in the center of the medium. Over time, as temperature increases both the pore water and the solid skeleton expand. Since in general the thermal expansion of water is greater than that of the solid medium, the pore pressure increases, which leads to a reduction in effective stresses (THM coupling). The pore pressure increase gradually dissipates as the medium is allowed to consolidate. Booker and Savvidou (1985) proposed analytical solutions for pore pressure, temperature, stresses and displacements for a constant point heat source embedded in an infinite medium. An approximate solution for a cylindrical source was also given. It should be noted that this problem is three-dimensional, but can be reduced to axisymmetric conditions assuming an isotropic elastic material.

Fig. 5 shows the model prepared to benchmark TOUGH-FLAC against the analytical solutions in Booker and Savvidou (1985). We note that, in order to reproduce an infinite medium, Dirichlet boundary conditions (i.e., constant pore pressure and temperature) are imposed at the outer boundaries of the model ( $R = Z = 200$  m in Fig. 5). The heat source is applied in a small element at  $r = z = 0$ . The medium is linear elastic with  $E=650$  MPa and  $\nu=0.24$ . The initial stress field is 0.1 MPa (compressive), equal to the initial pore pressure. The sample is saturated with water. The initial temperature is  $T_0 = 25$  °C, and we apply a heat source of 15.6 W. The initial porosity of the sample is  $\phi_0 = 45\%$ , its permeability is  $k=6.51 \cdot 10^{-18}$  m<sup>2</sup>, its thermal conductivity is  $\lambda=1.2$  W/m/K, and the coefficient of linear thermal expansion is  $\alpha_{th} = 7 \cdot 10^{-6}$  K<sup>-1</sup>. Solid density is  $\rho=2500$  kg/m<sup>3</sup> and the specific heat of the solid skeleton is  $C_p=1000$  J/kg/K. Gravity is neglected.

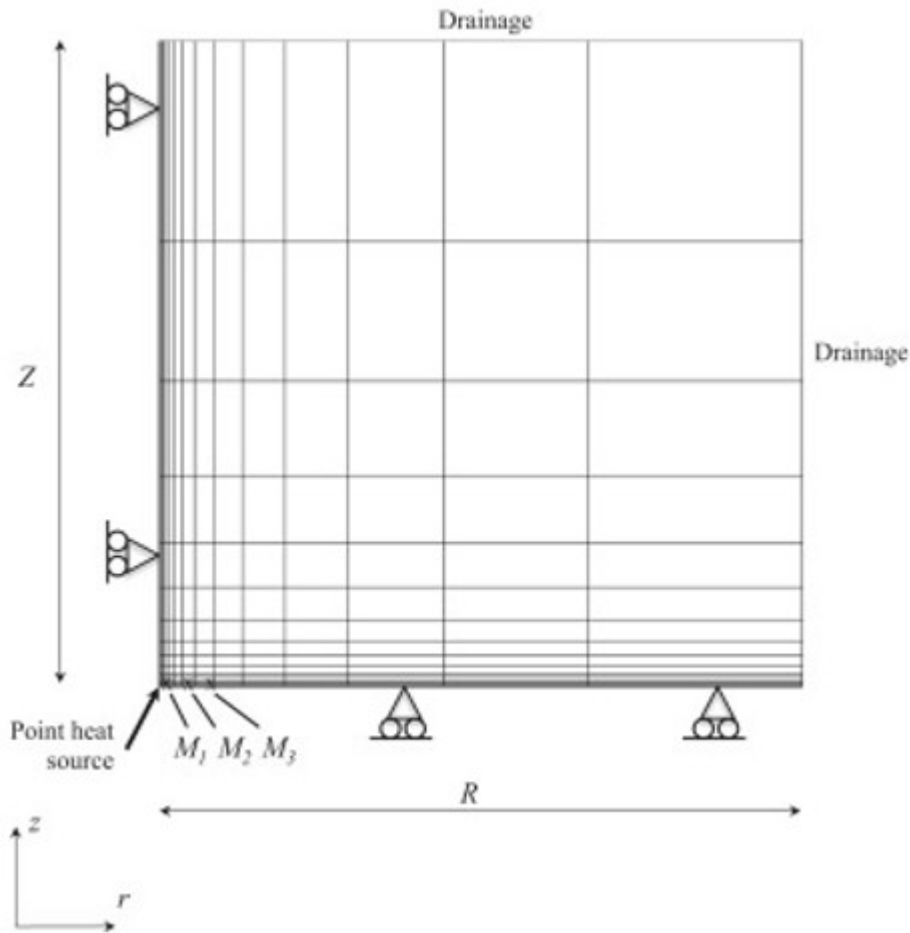


Fig. 5. Schematic representation of Booker and Savidou's problem. Monitoring points ( $M_1$ ,  $M_2$  and  $M_3$ ) for Fig. 6 are indicated (they are all located along the radial axis).

Fig. 6a compares analytical and modeling results for temperature at three locations along the radial axis of the model. The pore pressure evolution at these locations is displayed in Fig. 6b. As the figures show, results from TOUGH-FLAC compare quite well with the analytical solutions, with biggest errors at shorter distances from the heat source (in TOUGH-FLAC, the heat load is applied to a small-volume element rather than to a point).

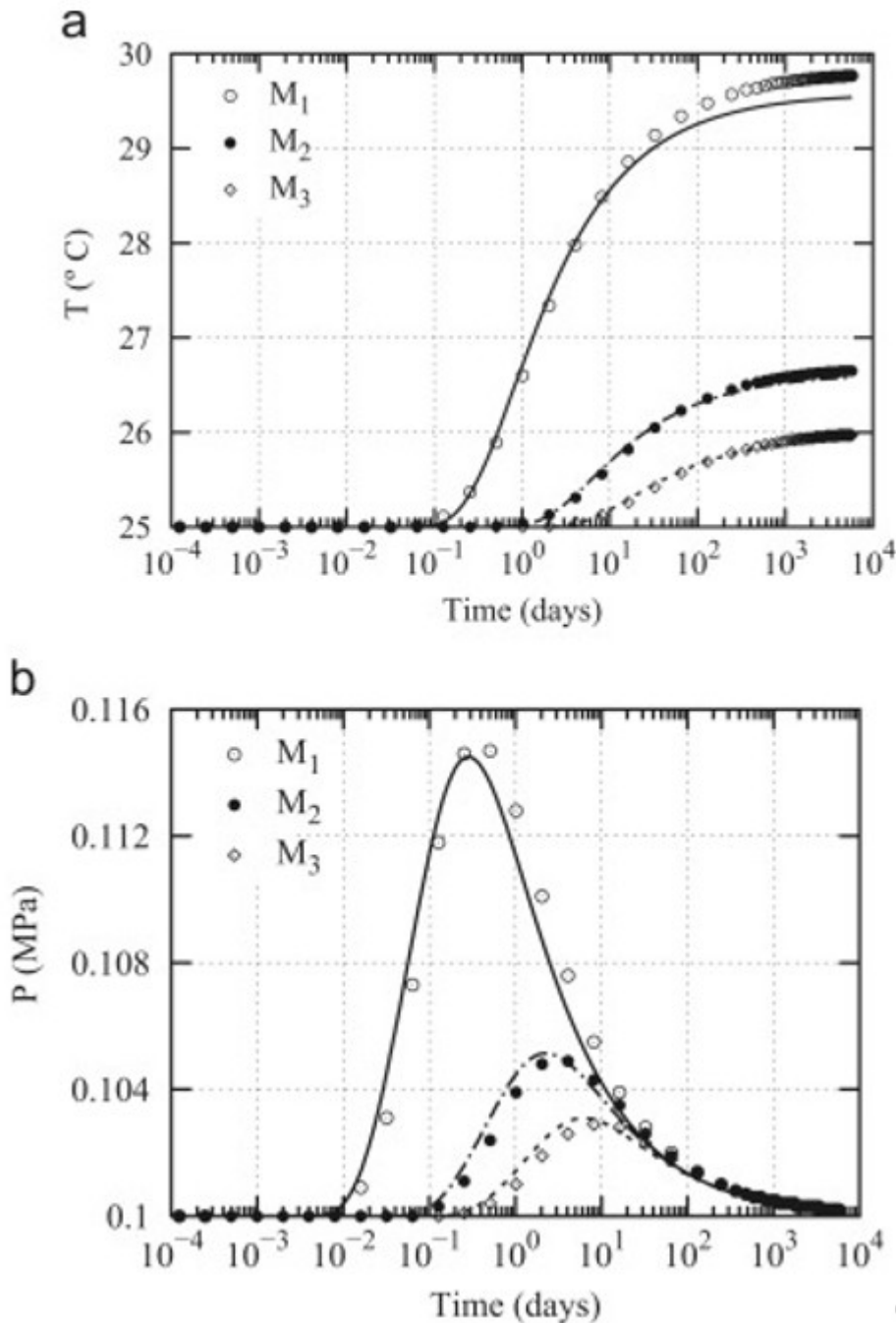


Fig. 6. Booker and Savidou's problem: comparison between analytical (lines) and modeling (symbols) results for (a) temperature, and (b) pore pressure at locations  $M_1=0.22$  m,  $M_2=0.63$  m, and  $M_3=1$  m.

### 3.3. Terzaghi's problem (small strains)

Terzaghi's problem (Terzaghi, 1943) is a classic consolidation problem. It is a one-dimensional problem, in which a compressive load is applied on one side of a sample while the displacement normal to the other sides is blocked. The pore space is in single-phase conditions, and drainage is only allowed across

the side where the load is applied. Fig. 7 shows schematically Terzaghi's problem.

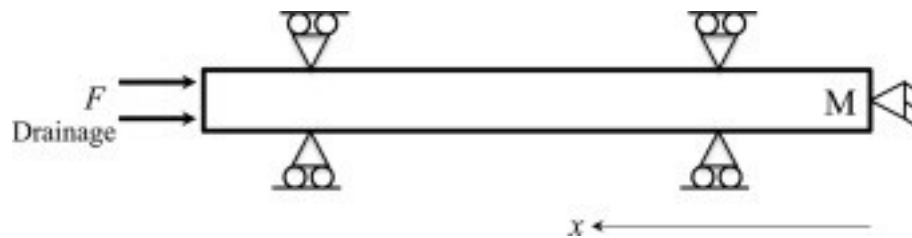


Fig. 7. Schematic representation of Terzaghi's problem. The monitoring point ( $M$ ) for Fig. 8, Fig. 9, Fig. 11 is displayed.

Similarly to Mandel's problem, when the load is applied the pore pressure increases (Skempton effect) and then the excess of pore pressure dissipates as the fluid flows out of the sample. One the other hand, one main difference with Mandel's problem is that, in Terzaghi's problem, the load and the dissipation of pore pressure occur in the same direction. Moreover, the total stress is constant along the sample, and is equal to the applied load. Therefore, as the fluid flows out of the sample and the pore pressure decreases, there is a load transfer between the fluid and the solid, so that the effective stresses increase. We note that in Terzaghi's problem the pore pressure decreases monotonically after the initial rise, and therefore the Mandel-Cryer effect, distinctive feature of the coupled consolidation theory, is not observed.

Terzaghi's problem has been modeled with TOUGH-FLAC, using  $L = 31$  m,  $E = 600$  MPa, and  $\nu = 0.15$ . Initially, the sample is in equilibrium under a compressive stress of 10 MPa (the initial pore pressure is also 10 MPa). The initial porosity is  $\phi_0 = 42.5\%$  and the permeability of the sample is  $k = 6.5 \cdot 10^{-15}$  m<sup>2</sup>. The sample is saturated with water, having  $T = 25$  °C (constant). At  $t = 0$ , the applied load increases by 10 MPa. Gravity is neglected. The plots in Fig. 8 show a comparison between analytical and modeling results for the evolution of pore pressure at the monitoring point  $M$  (0.5 m from the right border). In Fig. 8a, the water is assumed incompressible and in Fig. 8b, real water compressibility is used. The latter corresponds to the standard procedure in TOUGH2; to obtain the modeling results in Fig. 8a, water compressibility in TOUGH2 is forced constant at a near-zero value. As Fig. 8a shows, if the water is assumed incompressible the initial pore pressure increase is equal to the applied load (i.e., the fluid bears the load initially), while it is about 1 MPa smaller if the real compressibility of water is used. In both cases, the pressure dissipation over time is very well captured by TOUGH-FLAC. We note that, similarly to Mandel's problem, the initial state is different between the analytical solution and TOUGH-FLAC.

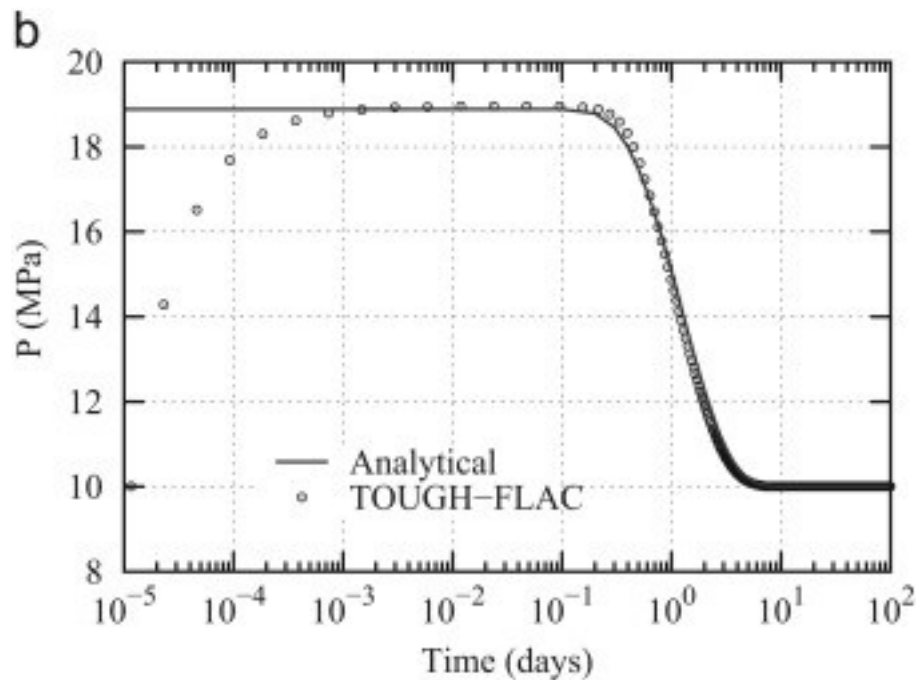
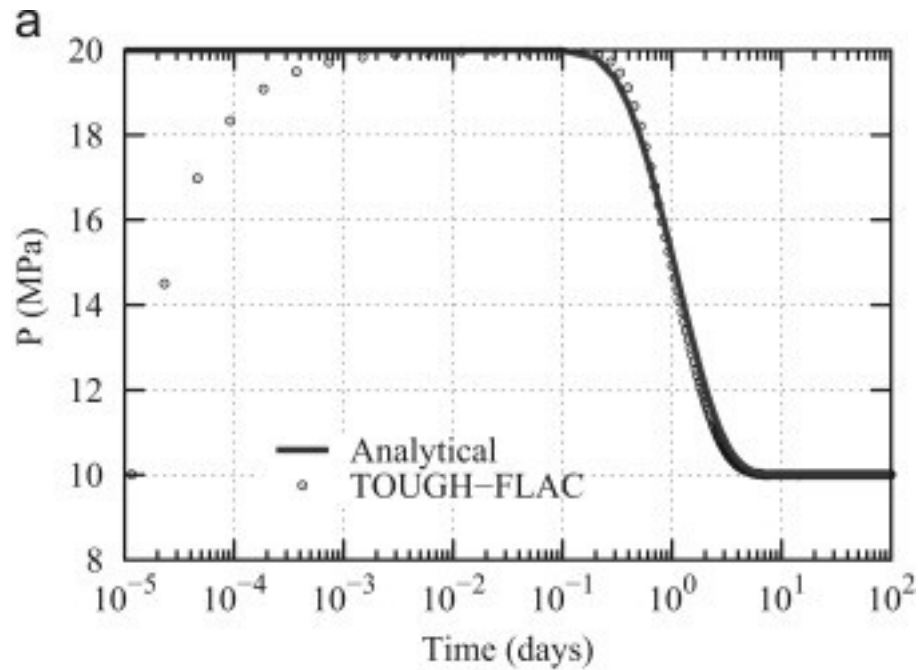


Fig. 8. Terzaghi's problem (infinitesimal strains): comparison between analytical and modeled pore pressure evolution at the monitoring point, for (a) incompressible water, and (b) real water compressibility.

### 3.4. Terzaghi's problem (large strains)

In order to test the validity of TOUGH-FLAC in finite strains, we compare results from this simulator with results issued from other approaches and codes that can handle large strains.



Kim (2015) presents an approach based on the total Lagrangian method to sequentially couple flow and geomechanics in finite strains. In this method, geometry is not updated, and instead pertinent properties are mapped onto a reference configuration (original). As explained in Section 2.2, the main advantage of this method is that the recalculation of geometry is not needed (therefore, the computational cost is reduced), and the main drawback is the need for full permeability tensors, not implemented in standard versions of various flow simulators, including TOUGH2.

In Kim (2015), the total Lagrangian method is applied to Terzaghi's problem. The same scenario has been solved with TOUGH-FLAC. In this case,  $L = 31$  m,  $E = 60$  MPa, and  $\nu = 0.15$ . The initial compressive total stress and pore pressure are 8.3 MPa, and at  $t=0$  the applied load increases by 8.3 MPa. The initial porosity is  $\phi_0 = 42.5\%$  and the permeability of the sample is  $k = 6.5 \cdot 10^{-15}$  m<sup>2</sup> ( $T = 25$  °C). Gravity is neglected. In Fig. 9, results from TOUGH-FLAC and Kim (2015) are shown; as the figure shows, the comparison is very satisfactory. Three views of the mesh during the TOUGH-FLAC simulation are displayed in Fig. 10. As it can be seen, there has been a significant geometrical change, with volume evolution from 31 m<sup>3</sup> ( $t=0$ ) to 27 m<sup>3</sup> ( $t=500$  days).

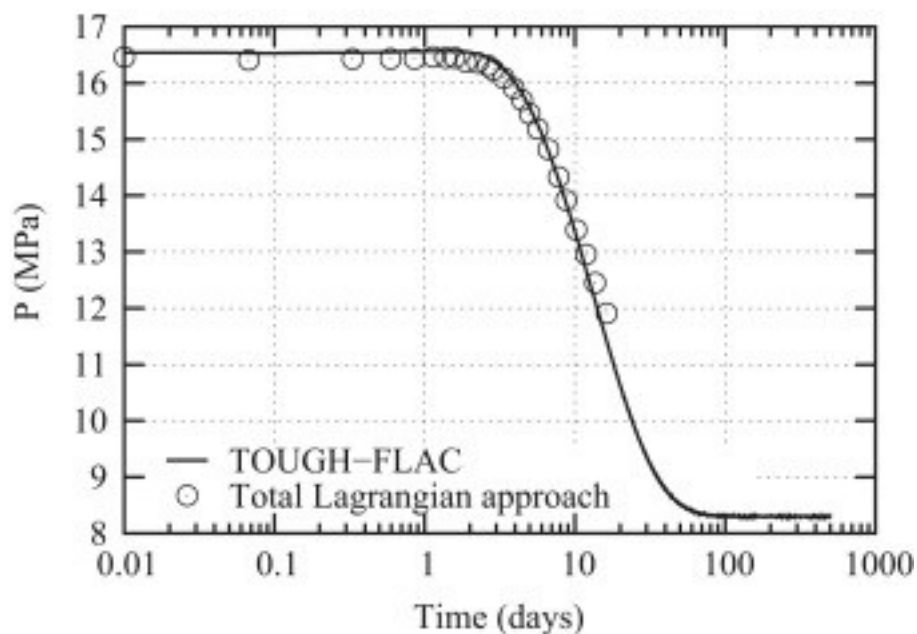


Fig. 9. Terzaghi's problem (finite strains): comparison between results from TOUGH-FLAC and those in Kim (2015) for the pore pressure evolution at the monitoring point.

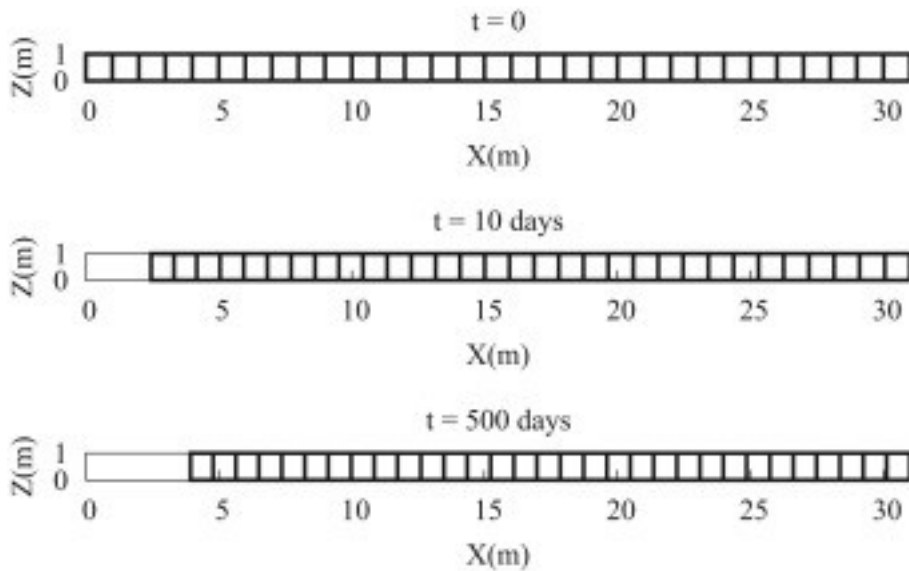


Fig. 10. Terzaghi's problem (finite strains): view of the mesh at  $t=0$ ,  $t=10$  days, and  $t=500$  days (end of simulation).

Finally, in order to demonstrate the relevance of the large strain framework, the same case presented has been solved using small strains. The pore pressure evolution obtained in the two situations at location  $M$  is displayed in Fig. 11. It can be seen that when the problem is solved in small strains the pore pressure dissipates faster; however, this result is not general because it depends on the counteracting effects in finite strains of compressibility reduction (which reduces deformation) and diffusion length reduction (which facilitates consolidation). Moreover, it should be noted that, since the mesh is very small (31 grid-blocks), the computational times of the two simulations are approximately equal.

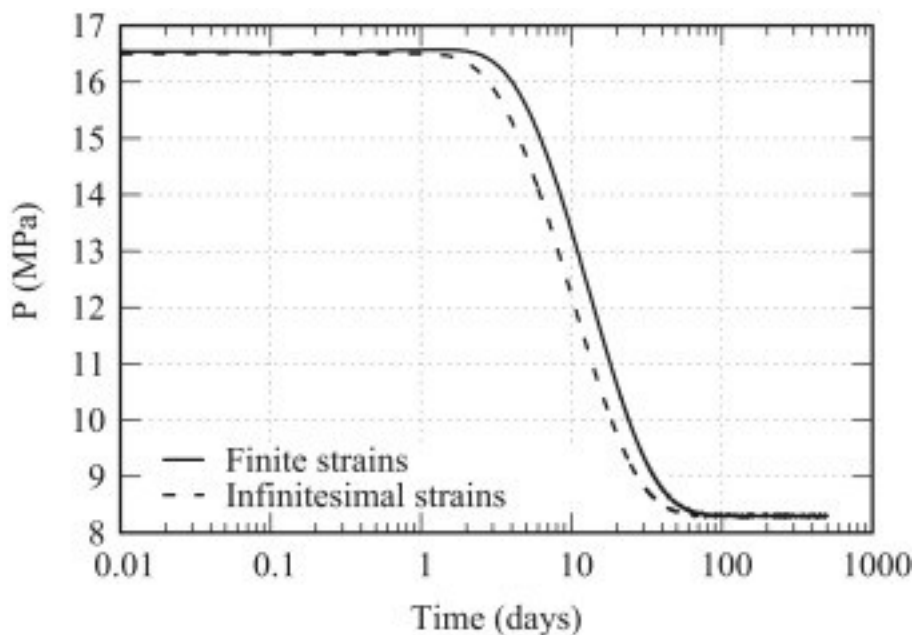


Fig. 11. Terzaghi's problem: pore pressure evolution at the monitoring point under the infinitesimal and the finite strain frameworks.

#### 4. Field scale application: disposal of heat-generating nuclear waste in rock salt

TOUGH-FLAC in finite strains and creep modes has been used to model a large-scale underground heater test conducted in the Asse salt mine in Germany (Blanco-Martín et al., 2016). The goal of this test (Thermal Simulation for Drift Emplacement, or TSDE) was to investigate the feasibility of disposal of heat-generating nuclear waste in a rock salt formation, using crushed salt backfilling (Bechthold et al., 1999, Bechthold et al., 2004). The fundamentals of disposal of heat-generating nuclear waste in salt-based formations can be found in, e.g., Hansen and Leigh (2011), and Langer (1999). Details on the modeling of rock salt and salt excavations can be found in, e.g., Cristescu and Hunsche (1996), Hou and Lux (1999), Hunsche et al., (1994), Hunsche and Hampel (1999), and Munson (1997).

During the TSDE test, heating was provided by six electrical heaters placed in two 79 m-long parallel drifts. The heaters (three per drift) were placed in the central part of the drifts, spaced 3 m along the drift axis. The heating period lasted 8 years and 5 months, and an extensive measurement campaign was deployed to study the host rock, the backfill and also the corrosion of the heater casks.

Fig. 12 compares experimental and computed backfill porosity in two cross-sections in the heated area of one drift. Experimental porosity was derived from horizontal and vertical drift closure measurements (Bechthold et al., 1999). At emplacement, the porosity of the crushed salt was 35%, and it decreased to about 24–26% during the heating phase. Given the porosity reduction observed (about 10%), the finite strain framework was selected for the numerical analysis (details of this analysis can be found in Blanco-Martín et al., 2016). The figure displays a good agreement between experimental data and modeling results from TOUGH-FLAC. Although the experimental values are only approximate (they are average values within a cross-section), this comparison shows that TOUGH-FLAC can be successfully applied to a large-scale application involving finite strains and time-dependent rheology.

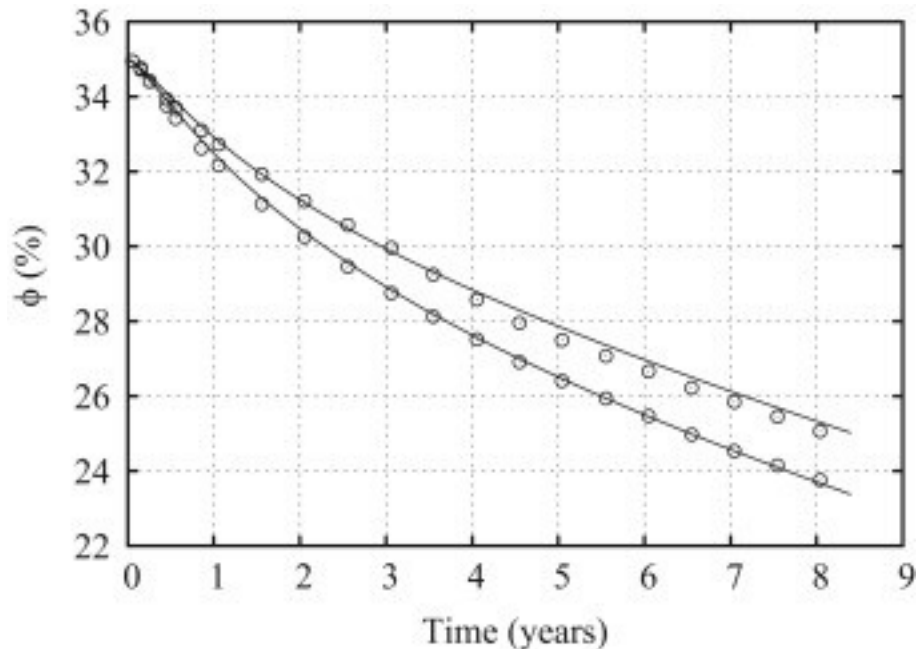


Fig. 12. Porosity evolution at two cross-sections in the heated part of a test drift during the TSDE experiment: comparison between measurements (symbols) and modeling results (lines).

## 5. Conclusions

The simulator TOUGH-FLAC for coupled thermal-hydraulic-mechanical processes modeling has been extended to the finite strain framework. Since FLAC<sup>3D</sup> includes a capability for finite strains, the main modifications to TOUGH-FLAC have concerned the flow simulator (TOUGH2) and the coupling scheme between the two codes.

The approach selected consists in updating the geometry of the flow sub-problem as finite strains are computed in the geomechanics sub-problem. In TOUGH2, the mass and energy balance equations have been extended to account for volume changes. Moreover, all geometrical data (volumes, areas, distances, etc.) are updated during the simulation. Since the resolution method used in TOUGH2 is based on the Voronoi partition, a new Voronoi diagram is computed every time geometrical changes exceed a preset limit. The centroids of the deformed geomechanics mesh are sent to Vorop++ (open source library that computes Voronoi diagrams given seed points), and geometrical data of the new partition is sent to TOUGH2 for the next time step. The update of geometrical data is carried out internally and the impact to the user is very limited, as only one additional executable (Voro++) is needed to perform a simulation.

TOUGH-FLAC has been verified against analytical solutions of Terzaghi, Booker and Savvidou, and Mandel's problems. In finite strains, this simulator has been successfully benchmarked against other approaches to perform large strain computations of coupled flow and geomechanics problems. A large-scale heater test designed to study the feasibility of disposal of heat-

generating nuclear waste in rock salt formations using crushed salt backfilling has also been successfully modeled using this new version of TOUGH-FLAC.

The extension of TOUGH-FLAC to the large strain framework expands its use to the analysis of a variety of engineering problems, and therefore broadens its current areas of application.

#### Acknowledgements

Funding for this work has been provided by the Used Fuel Disposition Campaign, Office of Nuclear Energy of the U.S. Department of Energy, under Contract Number DE-AC02-05CH11231 with Lawrence Berkeley National Laboratory.

#### References

- Abousleiman et al., 1996 Y. Abousleiman, A.H.-  
D. Cheng, L. Cui, E. Detournay, J.-C. Roegiers **Mandel's problem revisited** Géotechnique, 46 (2) (1996), pp. 187-195, 10.1680/geot.1996.46.2.187
- W. Bechthold, T. Rothfuchs, A. Poley, M. Ghoreychi, S. Heusermann, A. Gens, S. Olivella **Backfilling and sealing of underground repositories for radioactive waste in salt (BAMBUS project)** Eur. At. Energy Community (1999), p. 283
- W. Bechthold, E. Smailos, S. Heusermann, W. Bollingerfehr, B. Bazargan-Sabet, T. Rothfuchs, P. Kamlot, J. Grupa, S. Olivella, F.D. Hansen **Backfilling and sealing of underground repositories for radioactive waste in salt (BAMBUS II project)** Eur. At. Energy Community (2004), p. 305
- Blanco-Martín, L., Rutqvist, J., Birkholzer, J.T., 2015a. Extension of the TOUGH-FLAC simulator to account for finite strains. In: Proceedings of TOUGH Symposium, Berkeley, CA, pp. 266-271
- L. Blanco-Martín, J. Rutqvist, J.T. Birkholzer **Long-term modelling of the thermal-hydraulic-mechanical response of a generic salt repository for heat generating nuclear waste** Eng. Geol., 193 (2015), pp. 198-211, 10.1016/j.enggeo.2015.04.014
- L. Blanco-Martín, R. Wolters, J. Rutqvist, K.-H. Lux, J.T. Birkholzer **Thermal-hydraulic-mechanical modeling of a large-scale heater test to investigate rock salt and crushed salt behavior under repository conditions for heat-generating nuclear waste** Comput. Geotech., 77 (2016), pp. 120-133, 10.1016/j.compgeo.2016.04.008
- J.R. Booker, C. Savvidou **Consolidation around a point heat source** Int. J. Numer. Anal. Methods Geomech., 9 (1985), pp. 173-184, 10.1002/nag.1610090206
- Cristescu, N., Hunsche, U., 1996. A comprehensive equation for rock salt: determination and application. In: Proceedings of the 3rd International Conference Mechanical Behavior of Rock Salt (SaltMech3), Palaiseau, pp. 191-205.

R.H. Dean, X. Gai, C.M. Stone, S.E. Minkoff **A comparison of techniques for coupling porous flow and geomechanics** SPE J., 11 (1) (2006), pp. 132-140, 10.2118/79709-PA

F.D. Hansen, C.D. Leigh **Salt Disposal of Heat-Generating Nuclear Waste** Sandia National Laboratories (2011), p. 110

U. Hunsche, A. Hampel **Rock salt - the mechanical properties of the host rock material for a radioactive waste repository** Eng. Geol., 52 (1999), pp. 271-291, 10.1016/S0013-7952(99)00011-3

Hunsche, U., Schulze, O., Langer, M., 1994. Creep and failure behavior of rock salt around underground cavities. In: Proceedings 16th World Mining Congress, vol. 5, Sofia, pp. 217-230.

Itasca **FLAC<sup>3D</sup> (Fast Lagrangian Analysis of Continua in 3 Dimensions), Version 5.0** Itasca Consulting Group, Minneapolis, MN (2012)

Kim, J., Tchelepi, H.A., Juanes, R., 2009. Stability, Accuracy and Efficiency of Sequential Methods for Coupled Flow and Geomechanics. In: SPE Reservoir Simulation Symposium, The Woodlands, TX, paper SPE 119084. <http://dx.doi.org/10.2118/119084-MS>

J. Kim, E.L. Sonnenthal, J. Rutqvist **Formulation and sequential numerical algorithms of coupled fluid/heat flow and geomechanics for multiple porosity materials** Int. J. Numer. Methods Eng., 92 (5) (2012), pp. 425-456, 10.1002/nme.4340

Kim, J., 2015. A Numerically Stable Sequential Implicit Algorithm for Finite-strain Elastoplastic Geomechanics Coupled to Fluid Flow. In: SPE Reservoir Simulation Symposium, Houston, TX, paper SPE 173303. <http://dx.doi.org/10.2118/173303-MS>

Kröhn, K.-P., Zhang, C.-L., Czaikowski, O., Stührenberg, D., Heemann, U., 2015. The compaction behaviour of salt backfill as a THM-process. In: Proceedings of the 8th International Conference Mechanical Behavior of Salt (SaltMech8), Rapid City, pp. 49-59. <http://dx.doi.org/10.1201/b18393-8>

Hou, Z., Lux, K.-H., 1999. A constitutive model for rock salt including structural damages as well as practice-oriented applications. In: Proceedings of the 5th International Conference Mechanical Behavior of Rock Salt (SaltMech5), Bucharest, pp. 151-169.

M. Langer **Principles of geomechanical safety assessment for radioactive waste disposal in salt structures** Eng. Geol., 52 (1999), pp. 257-269, 10.1016/S0013-7952(99)00010-1

J. Mandel **La consolidation des sols (étude mathématique)** Géotechnique, 3 (7) (1953), pp. 287-299, 10.1680/geot.1953.3.7.287

G.J. Moridis, J. Kim, M.T. Reagan, S.-J. Kim **Feasibility of gas production from a gas hydrate accumulation at the UBGH2-6 site of the Ulleung**

**basin in the Korean East Sea** J. Pet. Sci. Eng., 108 (2013), pp. 180-210, 10.1016/j.petrol.2013.03.002

D.E. Munson **Constitutive model of creep in rock salt applied to underground room closure** Int. J. Rock. Mech. Min. Sci., 34 (2) (1997), pp. 233-247, 10.1016/S0148-9062(96)00047-2

T.S. Nguyen, A.P.S. Selvadurai **Coupled thermal-mechanical-hydrological behaviour of sparsely fractured rock: implications for nuclear waste disposal** Int. J. Rock. Mech. Min. Sci., 32 (5) (1995), pp. 465-479, 10.1016/0148-9062(95)00036-G

K. Pruess, C. Oldenburg, G.J. Moridis **TOUGH2 User's Guide, Version 2.1** Lawrence Berkeley National Laboratory (2012), p. 210

J. Rutqvist, Y.-S. Wu, C.-F. Tsang, G. Bodvarsson **A modeling approach for analysis of coupled multiphase fluid flow, heat transfer, and deformation in fractured porous rock** Int. J. Rock. Mech. Min. Sci., 39 (4) (2002), pp. 429-442, 10.1016/S1365-1609%2802%2900022-9

Rutqvist, J., Tsang, C.-F., 2003. TOUGH-FLAC: a numerical simulator for analysis of coupled thermal-hydrologic-mechanical processes in fractured and porous geological media under multi-phase flow conditions. In: Proceedings TOUGH Symposium, Berkeley, CA, 9 pp.

J. Rutqvist **Status of the TOUGH-FLAC simulator and recent applications related to coupled fluid flow and crustal deformations** Comput. Geosci., 37 (2011), pp. 739-750, 10.1016/j.cageo.2010.08.006

Rutqvist, J., 2015. An overview of TOUGH-based geomechanics models. In: Proceedings TOUGH Symposium, Berkeley, CA, pp. 301-313.

C.H. Rycroft Voro++: a three-Dimens. Voronoi Cell Libr. C++ (2009) <http://math.lbl.gov/voro++/>

A. Settari, F. Mourits **A coupled reservoir and geomechanical simulation system** SPE J., 3 (3) (1998), pp. 219-226, 10.2118/50939-PA

R.L. Schiffman, A.T.-F. Chen, J.C. Jordan **An analysis of consolidation theories** J. Soil Mech. Found. Div., 95 (1) (1969), pp. 285-312

K. Terzaghi **Theoretical Soil Mechanics** John Wiley & Sons, New York, NY (1943), p. 510, 10.1002/9780470172766

A. Verruijt **Elastic storage of aquifers** R.J.M. De Wiest (Ed.), Flow through Porous Media, Academic Press, New York (1969), pp. 331-376